Identity, developmental restriction and reactivity of extralaminar cells capping mammalian neuromuscular junctions

Felipe A. Court[1,2,*], Thomas H. Gillingwater[1,2], Shona Melrose[2], Diane L. Sherman[2], Kay N. Greenshields[3], A. Jennifer Morton[4], John B. Harris[5] Hugh J. Willison[3] and Richard R. Ribchester[1,2,‡]

[1]Euan MacDonald Centre for Motor Neurone Disease Research, The University of Edinburgh, 1 George Square, Edinburgh EH8 9JZ, UK
[2]Centre for Neuroscience Research, The University of Edinburgh, Summerhall, Edinburgh EH9 1QH, UK
[3]Division of Clinical Neuroscience, Glasgow Biomedical Research Centre, University of Glasgow, 120 University Place, Glasgow G12 8TA, UK
[4]Department of Pharmacology, University of Cambridge, Tennis Court Road, Cambridge CB2 1PD, UK
[5]Institute of Neuroscience Faculty of Medical Sciences, University of Newcastle upon Tyne, Framlington Place, Newcastle upon Tyne NE2 4HH, UK

*Present address: Department of Physiological Sciences, Faculty of Biology, P. Universidad Católica de Chile, Av. B. O'Higgins 340, Casilla 114-D, Santiago, Chile
‡Author for correspondence (e-mail: richard.ribchester@ed.ac.uk)

Summary

Neuromuscular junctions (NMJs) are normally thought to comprise three major cell types: skeletal muscle fibres, motor neuron terminals and perisynaptic terminal Schwann cells. Here we studied a fourth population of junctional cells in mice and rats, revealed using a novel cytoskeletal antibody (2166). These cells lie outside the synaptic basal lamina but form caps over NMJs during postnatal development. NMJ-capping cells also bound rPH, HM-24, CD34 antibodies and cholera toxin B subunit. Bromodeoxyuridine incorporation indicated activation, proliferation and spread of NMJ-capping cells following denervation in adults, in advance of terminal Schwann cell sprouting. The NMJ-capping cell reaction coincided with expression of tenascin-C but was independent of this molecule because capping cells also dispersed after denervation in tenascin-C-null mutant mice. NMJ-capping cells also dispersed after local paralysis with botulinum toxin and in atrophic muscles of transgenic R6/2 mice. We conclude that NMJ-capping cells (proposed name 'kranocytes') represent a neglected, canonical cellular constituent of neuromuscular junctions where they could play a permissive role in synaptic regeneration.

Introduction

Neuromuscular junctions (NMJs) are interfaces between components of two main cell types: motor axon terminals and motor endplates of skeletal muscle fibres. In adult mammals and most other vertebrates, each motor endplate is normally innervated by a single motor axon terminal and in most muscle fibres this NMJ is constrained to less than 0.1% of the muscle fibre cell surface (Sanes and Lichtman, 1999; Beeson et al., 2006). The strength of synaptic transmission at each NMJ in a motor unit virtually guarantees that all the muscle fibres supplied by a motor neuron contract in response to every action potential conducted into its motor nerve terminals (Wood and Slater, 2001). NMJs are therefore crucial structures in the intercellular signalling processes that control movement and behaviour. Degeneration of motor nerve terminals occurs rapidly after axon injury, axonal transport block or neuromuscular paralysis (Miledi and Slater, 1970; Brown et al., 1980; Hudson et al., 1984) and in early stages of motor neuron diseases, such as amyotrophic lateral sclerosis (ALS) (Fischer et al., 2004; Pun et al., 2006; David et al., 2007). Compensatory responses to such denervation include sprouting from intact neighbouring axons and regeneration of damaged axons (Brown and Ironton, 1978; Barry and Ribchester, 1995; Costanzo et al., 1999; Costanzo et al., 2000; Schaefer et al., 2005). Understanding the cellular organisation of NMJs and the mediators

of their plasticity is therefore important: not only for the insights it provides into fundamental cell biology but also for identifying suitable cellular and molecular targets for effective treatment for ALS and other neuromuscular diseases.

Motor neurons and muscle fibres are not the only cell types present at an NMJ. In the endplate region, myelinating Schwann cells ensheath intramuscular axon collaterals up to the last heminode of Ranvier, ensuring high-fidelity conduction of action potentials (Court et al., 2004). The nerve terminal itself is capped by non-myelinating terminal Schwann cells (Robertson, 1956; Birks et al., 1960; Kang et al., 2003; Hayworth et al., 2006). These cells are contained in a continuation of the synaptic basal lamina and cover motor terminal branches and synaptic boutons, in register with other pre- and postsynaptic specialisations. Although not essential for the initial formation of neuromuscular synapses, terminal Schwann cells are required for maintenance of preterminal axon structure and function during development; for long-term maintenance of neuromuscular transmission in adult life; and they appear to have a path-finding role in compensatory sprouting responses following nerve injury and repair (Jahromi et al., 1992; Son and Thompson, 1995; Trachtenberg and Thompson, 1996; Castonguay and Robitaille, 2001; Reddy et al., 2003; Court et al., 2008). Thus, together, motor nerve terminals, muscle fibres and terminal Schwann cells are generally considered the three essential cellular elements

that constitute the vertebrate neuromuscular junction (Sanes and Lichtman, 1999; Hughes et al., 2006).

Here we report strong association of a fourth cell type with NMJs. This arose from a serendipitous initial finding: whole-mount immunofluorescent staining of skeletal muscle with a novel polyclonal antibody (2166) produced vivid cytoskeletal labelling of a sub-set of cells capping the NMJ but lying outside the synaptic basal lamina. These NMJ-capping cells may correspond to 'endoneurial cells' first identified in the neighbourhood of NMJs in pioneering ultrastructural studies of the NMJ by Robertson (Robertson, 1956), or to cells of similar appearance referred to by Weis et al. (Weis et al., 1991) as 'perisynaptic fibroblasts'. However, the data here suggest a much tighter association of NMJ-capping cells than indicated by these previous studies. NMJ-capping cells become restricted to neuromuscular junctions during postnatal development; however, within 24 hours of denervation or paralysis in adults, they proliferate and spread throughout the perijunctional region, ahead of reactive sprouting of either terminal Schwann cells or regenerating motor axons. Taken together, these findings suggest that mammalian neuromuscular junctions comprise four cell types, not three, and that NMJ-capping cells should be considered as integral constituents of neuromuscular junctions.

Results

2166 antibody stains NMJ-capping cells

Antibody 2166 was raised in rabbits against an epitope of Tspan-2, an oligodendrocyte-specific tetraspanin protein of 25 kDa (Birling et al., 1999; Terada et al., 2002). The original intention was to use this antibody to map oligodendrocyte disposition and lineage in the brain. However, preliminary analysis using western blots suggested the antibody recognised a protein of 47 kDa, which was not Tspan-2 (see Materials and Methods). Immunostained sections of brain indicated that the antibody did not stain oligodendrocytes either. Since the potential utility of the 2166 antibody did not depend on knowledge of its primary antigen, we proceeded to test it for potential binding to other neural tissues, including neuromuscular junctions, mainly anticipating the possibility of peripheral myelin or terminal Schwann cell staining.

Remarkably, 2166 immunostaining of whole-mount preparations of the mouse triangularis sterni (TS) muscle revealed a subpopulation of cells, some of which were localised to neuromuscular junctions, where they formed caps over the motor nerve terminals. The 2166 antibody evidently stained the cytoskeleton in these capping cells (Fig. 1A-C; and see below) and frequently took the form of a lasso around the cell nucleus, appearing to extend into numerous filopodial or lamellipodial cellular processes. In most cases these extended over and beyond the boundaries of the motor endplate, as indicated by binding of rhodamine-conjugated α-bungarotoxin (TRITC-α-BTX), a specific ligand for postsynaptic acetylcholine (ACh) receptors. We subsequently observed 2166-positive cells capping neuromuscular junctions in several other skeletal muscles in mice and rats (diaphragm, soleus, extensor digitorum longus, flexor digitorum brevis and deep lumbricals). Thus, we refer to the NMJ-localised 2166-positive cells throughout the Results section of this report as 'NMJ-capping cells' (see Discussion for justification of a proposal to call them 'kranocytes').

Although the disposition of NMJ-capping cells was unequivocal, several other forms of 2166-immunopositive cells were observed beyond the junctional region in confocal micrographs, including the optical sections above and below the NMJs. However, there was only enrichment of 2166-positive cells in the vicinity of intramuscular
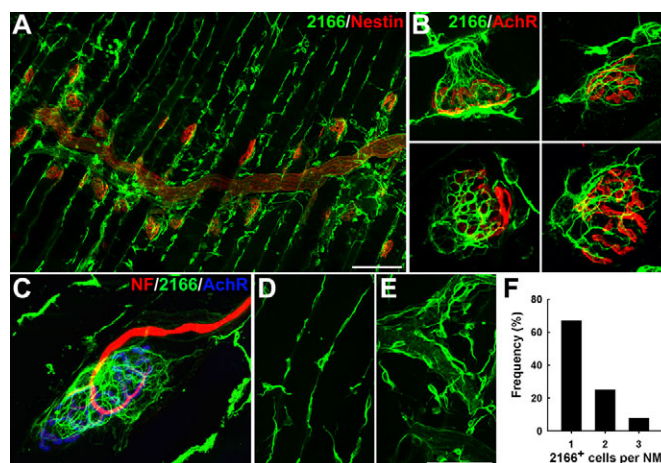

Fig. 1. Immunostaining of mouse triangularis sterni muscles with 2166 antibody reveals capping cells at NMJs. (A) Low-power confocal projection showing numerous 2166-positive interstitial cells and a prominent subpopulation in the vicinity of NMJs. (B) High-power confocal projection images of NMJ-capping cells (green), juxtaposed with motor endplates counterstained with TRITC-α-BTX (red). (C) Triple-stained NMJ with axon stained with neurofilament antibodies (red), NMJ-capping cell (green) and motor endplate AChR stained with Alexa Fluor 647-α-BTX (blue). (D,E) Other interstitial and endothelial cells with positive 2166 immunostaining were scattered at low density throughout the muscles. (F) Quantification of density of NMJ-capping cells at motor endplates. All endplates showed at least one and most were associated with only one NMJ-capping cell; no NMJ was associated with more than three of these cells. Scale bars: 100 μm (A); 20 μm (E, applies also to B-D).

nerves and in contrast to the morphology of NMJ-capping cells, virtually all of the 2166-positive extrajunctional cells had a bipolar form, with extensions running along the longitudinal axis of the muscle fibres (Fig. 1D). A similar bipolar form in 2166-positive cells was also associated with intramuscular capillaries (Fig. 1E).

The only clusters of capping cells were found around motor endplates. We counted the number of 2166-positive cells at neuromuscular junctions in adult TS muscles, counterstained with the nuclear marker DAPI (n=5 muscles, 100 neuromuscular junctions analysed). All neuromuscular junctions were capped by at least one 2166-positive cell. About 25% exhibited two, with fewer than 10% showing three (Fig. 1F). Outside the region of the NMJs, 2166-positive cells did not show any discernible clustering.

NMJ-capping cells show a distinct immunocytochemical profile

Immunocytochemical analysis (Table 1) clearly resolved NMJ-capping cells from terminal Schwann cells and suggested a distinct identity. First, double immunostaining with 2166 antibody and antibodies for either GFAP or nestin showed no colocalisation, demonstrating that NMJ-capping cells are not terminal Schwann cells. We confirmed this by 2166 immunostaining in S100-eGFP mice (Zuo et al., 2004) in which all myelinating and terminal Schwann cells are endogenously fluorescent (Fig. 2A). The 2166 immunostaining pattern was completely different and extended beyond the boundaries of the Schwann cell plasma membrane. Immunostaining for M-cadherin, neural cell adhesion molecule (N-CAM) or desmin also did not label NMJ-capping cells, suggesting that they were not muscle satellite cells (Sanes et al., 1986; Fukada et al., 2004). Finally, absence of F4/80 immunostaining appears to rule out any identity with macrophages (Austyn and Gordon, 1981).

Table 1. Panel of cellular and molecular markers used to screen for NMJ-capping-cell epitopes

Antibody/marker	Cell type or antigen	Antibody 2166 staining*
S100	Schwann cells	−
GFAP	Reactive Schwann cells	−
Nestin	Reactive Schwann cells	−
M-Cadherin	Satellite cells	−
NCAM	Satellite cells	−
Desmin	Satellite cells	−
Thy-1	Fibroblasts/neurons	−
F4/80	Macrophages	−
CD34	Stem cells	+
rPH	Fibroblasts	+
HM-24	GGFII-related molecules	+
CTB	GM1 ganglioside	+

*Positive staining was obtained with CD34, rPH, HM-24 and CTB. Other markers of Schwann cells, macrophages, fibroblasts and other satellite cells did not stain NMJ-capping cells.

We next examined whether NMJ-capping cells might be a specialised form of fibroblast. The exact disposition of 'perisynaptic fibroblasts' is unclear from previous reports, since they were depicted diagrammatically to be near to, but not overlying, neuromuscular junctions (Murray and Robbins, 1982; Gatchalian et al., 1989; Weis et al., 1991). No discernible immunofluorescence of NMJ-capping cells was detected using Thy-1 antibody, although axons, which also express Thy-1 antigen were immunolabelled (Reynolds and Woolf, 1992; Feng et al., 2000; Van der Putten et al., 2000). There were other Thy-1-positive cells near the NMJ but these did not include the 2166-positive NMJ-capping cells (supplementary material Fig. S1A). These positive controls confirmed the antibody specificity and affinity. Thus, 2166-positive cells may not correspond to the Thy-1-positive perisynaptic fibroblasts previously reported.

As a further test, we immunostained rat TS muscles using a mouse antibody against the rat isoform of prolyl-4-hydroxylase (rPH), an enzyme regulating the synthesis of collagen (Aiba et al., 1994; Smith et al., 1998). Positive staining for rPH was localised to 2166-positive cells above the NMJ although it did not overlap with 2166 immunostaining (Fig. 2B). Individual optical slices (Z-series) (supplementary material Movies 1 and 2) showed rPH and 2166 staining in the same cells. Thus, rPH is an enzyme evidently located in an intracellular compartment, possibly the endoplasmic reticulum (Nissi et al., 2001), near to but not overlapping the cytoskeletal components stained by 2166 antibody. Since 2166 antibody appeared to label specific cytoskeletal components, it is not surprising that it failed to colocalise with rPH. We did not examine whether rPH-positive fibroblasts in other tissues are also 2166 positive but it seemed clear that at least some cells with fibroblast-like characteristics also express the 2166 antigen.

The pattern of labelling of NMJ-capping cells suggests that the 2166 antigen is spatially quite restricted: for instance, there were substantial parts of cells, mostly near the periphery, where there was no 2166 labelling. To test whether the 2166 staining colocalised with other components of the cytoskeleton, we co-immunostained NMJ-capping cells with actin, vimentin or tubulin. The 2166 immunostaining was more restricted, with no strong colocalisation with these other cytoskeletal markers (data not shown).

Next, while searching cytological literature for evidence of NMJ-capping cell disposition, we noted the strong resemblance of 2166 antibody staining of the NMJ-capping cells to staining for neuregulin (GGFII) at NMJs, reported by Trinidad et al. (Trinidad et al., 2000). These authors used the HM-24 antibody and attributed the staining pattern to terminal Schwann cells. However, in our hands, HM-24 positive staining was not observed in S100-eGFP positive terminal Schwann cells (Fig. 2B). It was not possible to double-stain NMJ-capping cells with 2166 and HM-24 antibodies because both were raised in rabbits, but the HM-24 immunostaining pattern extended beyond the boundaries of the terminal Schwann cells. Interestingly, the pattern of HM-24 staining also appeared similar to the cytoskeletal labelling pattern of the 2166 antibody (Trinidad et al., 2000), which is perhaps surprising for neuregulin distribution. It is puzzling that these authors did not report seeing HM-24 staining in cells lying outside the synaptic basal lamina (see below). However, the present data suggest that junctional HM-24-positive cells appear to be identical to the NMJ-capping cells that we identified using the 2166 antibody.

Next, we looked for possible cell-surface markers of NMJ-capping cells. A stem cell population located in interstitial spaces of skeletal muscle, outside the basal lamina, has been identified previously and isolated by immunostaining for the hematopoietic stem cell marker CD34 (Torrente et al., 2001; Tamaki et al., 2002). We found that the surfaces of NMJ-capping cells showed uniform, faint immunostaining for CD34 (Fig. 3A,B). These preparations revealed additional aspects to the disposition of NMJ-capping cells: they frequently covered and extended beyond the NMJ and contacted the muscle fibre outside the end-plate perimeter, sometimes extending processes between adjacent motor endplates (Fig. 3B). This analysis also confirmed that the 2166 antigen was contained within the cytoskeletal framework of CD34-positive NMJ-capping cells. Orthogonal projections of the NMJ-capping cell showed that they were separated from the muscle fibre surface by about 3 μm and therefore that they were located outside the synaptic basal lamina (Fig. 3B; supplementary material Fig. S2). We
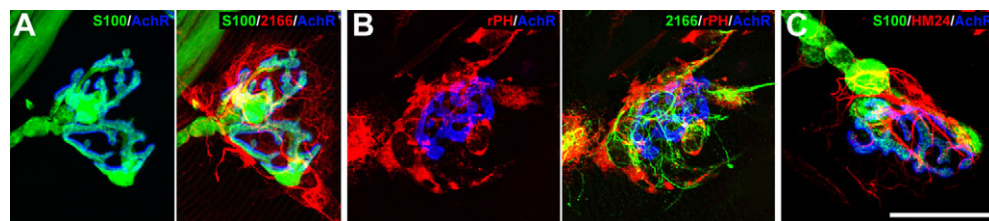

Fig. 2. NMJ-capping cells are not Schwann cells but express collagen-synthesising enzyme and neuregulin. (A) Confocal projection images of a TS muscle endplate in an S100-eGFP transgenic mouse, showing endogenous fluorescence in terminal Schwann cells (green) overlying endplate ACh receptors (blue). The right panel shows superimposition of 2166 immunostaining (red). (B) Immunostaining for the collagen-synthesising enzyme rPH of an NMJ-capping cell in rat TS muscle. (C) Immunostaining of a NMJ-capping cell in mouse triangularis sterni muscle using HM-24 antibody, which recognises GGFII/neuregulin. Scale bar: 50 μm.
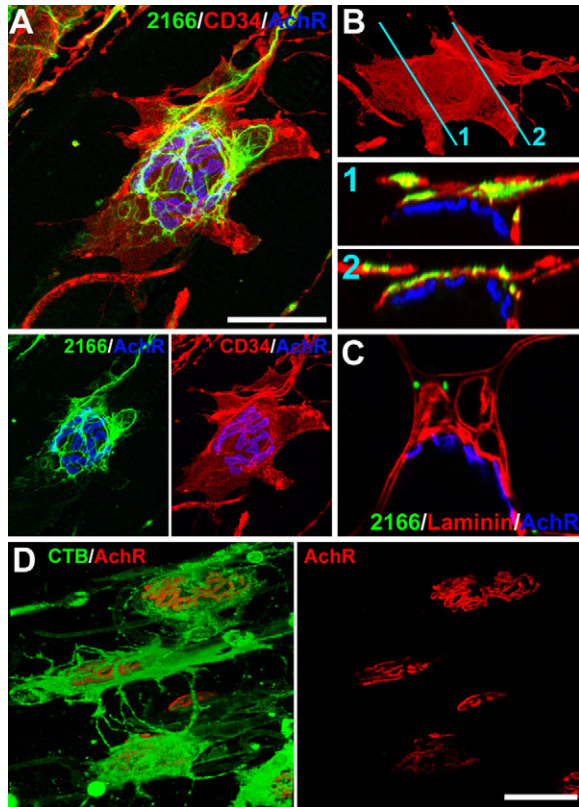
Fig. 3. NMJ-capping cells are positive for CD34 antibody and CTB and reside outside the synaptic basal lamina. (A,B) Confocal projections of an NMJ-capping cell in a mouse triangularis sterni muscle immunostained with 2166 (green) and CD34 (red) antibodies and with endplate AChR counterstained (blue). Lower panels in A show green and red channels separately; Panels 1 and 2 in B show orthogonal projections at the optical cuts indicated in the uppermost panel. (C) Transverse section of a mouse TS muscle immunostained with 2166 antibody (green spots), laminin antibody (red) and endplate ACh receptor (blue). The immunostained processes of the NMJ-capping cells clearly lie outside the basal lamina. (D) Fluorescent conjugates of CTB also stain cells similar in form and location to NMJ-capping cells. Right panel shows the red channel indicating endplate ACh receptors only. Scale bars: 50 μm.

confirmed this in transverse muscle sections co-immunostained with anti-laminin and 2166 antibodies, together with TRITC-α-BTX staining of ACh receptors (Fig. 3C).

Finally, we found that fluorescent conjugates of cholera toxin B subunit (CTB) highlighted the plasma membranes of NMJ-capping cells (Fig. 3D). We chose this reagent because it binds to GM1 gangliosides, which are absent from terminal Schwann cells (Halstead et al., 2005). Similarly to CD34 staining, membrane staining with CTB extended beyond the cytoskeletal staining with 2166 and also revealed several instances of fine cellular processes extending between motor endplates (supplementary material Movies 3-5). We did not attempt double labelling with CD34 antibody and CTB but they did appear to have a similar distribution pattern.

Ultrastructural disposition of NMJ-capping cells

We noted that many electron micrographs of NMJs in textbooks (e.g. Peters et al., 1991) crop images of NMJs to exclude cells other than terminal Schwann cells, nerve terminals and muscle fibres. However, original published transmission electron micrographs of NMJs in frogs, lizards, chickens, mice, rats and humans frequently

show slender cellular processes overlying the other principal cell types of the NMJ (Robertson, 1956; Desaki and Uehara, 1981; Connor and McMahan, 1987; Slater et al., 1992; Connor, 1997) (see also Fig. 4D). Thus, to extend the confocal microscopy data above, we made electron micrographs from 300 ultrathin (75-100 nm) serial sections of one randomly selected NMJ in a mouse TS muscle. We highlighted the profiles of the muscle fibre, motor nerve terminal, terminal Schwann cells and two putative NMJ-capping cells identified at this NMJ (Fig. 4A,B).

Volume rendering of a three-dimensional (3D) reconstruction of all of these cellular components confirmed the shape and relationship of the NMJ-capping cells with the other cellular components of the NMJ, as observed using light microscopy (Fig. 4C; supplementary material Movies 6 and 7). For example, the EM reconstruction confirmed the impression from confocal microscopy, indicating that the cellular processes of NMJ-capping cells are quite laminar.

Confocal microscopy suggested that NMJ-capping cells lack a basal lamina (see Fig. 3C). However, micrographs such as that shown in Fig. 4D indicate that capping cells are tightly ensheathed by a thin layer of extracellular matrix (see also supplementary material Fig. S3). Previous studies suggest that perisynaptic fibroblasts are also rich in endoplasmic reticulum. This appears also to be the case, at least for the capping cell shown in Fig. 4D and supplementary material Fig. S3.

In summary, whether NMJ-capping cells are identical to 'perisynaptic fibroblasts' described previously by others remains open. The data reported above suggest that NMJ-capping cells represent a distinct subpopulation of cells, defined by their shape, strong association with neuromuscular junctions and a distinctive molecular profile, as indicated by staining with a unique combination of five cytological markers: 2166, rPH, HM-24, CD34 and CTB.

Development and plasticity of NMJ-capping cells

The remarkable localisation of NMJ-capping cells, revealed here both by light microscopy of whole-mounts and by their reconstruction from electron micrographs, naturally led us to enquire about their possible functions. We focused initially on the patterns of 2166 immunostaining during early postnatal development and then we studied the effects of muscle atrophy, induced either by denervation, paralysis or disease. Finally, we investigated an association with tenascin-C, an early molecular marker of denervation, seeking insight into the possible mechanism of NMJ-capping cell plasticity.

2166-positive cells become restricted to NMJs postnatally

We immunostained TS muscles of postnatal mice aged 1-28 days (P1-P28). Neuromuscular junctions in these preparations were co-stained using neurofilament antibodies and fluorescent TRITC-α-BTX. At P1, 2166-positive cells were homogenously distributed along the TS muscle with no clear pattern of localisation to NMJs (Fig. 5A). Between P5 and P10, 2166-positive cells became more restricted to endplate bands adjacent to intramuscular nerve branches, but the degree of refinement between these times was not compelling (Fig. 5B-C). The pattern changed dramatically after P10, and by P28, 2166-positive cells were highly restricted to the neuromuscular junctions, as shown in Figs 1-3.

2166-positive cells spread after denervation, paralysis or muscle atrophy

Next, we partially denervated TS muscles in adult mice, then immunostained them 1-6 days later with nestin antibody, a marker
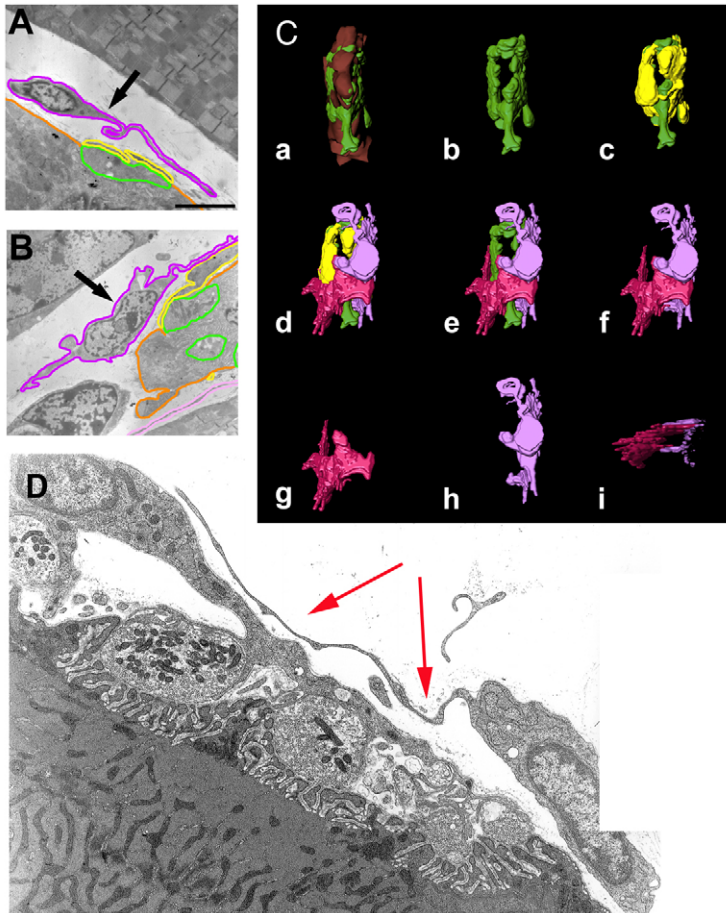
Fig. 4. NMJ-capping cells almost completely cover motor endplates. Electron micrographs and 3D surface-rendered reconstructions of serially sectioned electron micrographs showing the relationship between two putative NMJ-capping cells, motor nerve terminal, terminal Schwann cell and skeletal muscle fibre at a neuromuscular junction from mouse TS muscle. (A,B) Sections 84 and 75, respectively, from a 300-section series through a single NMJ. The soma and thin cytoplasmic processes of both NMJ-capping cells at this NMJ can be seen above the terminal Schwann cell and nerve terminal, lying outside the basal lamina. Each of the main cell types has been outlined on these electron micrographs (motor nerve terminal, green; muscle fibre, brown, terminal Schwann cell, yellow; 2166-positive cells, magenta and lilac). (C) Surface rendering of reconstructed serial electron micrographs from the NMJ shown in A and B revealed two NMJ-capping cells (magenta and lilac) overlying a single terminal Schwann cell (yellow) and a motor nerve terminal (green) synapsing with a skeletal muscle fibre (brown). a, Superior view of the nerve terminal and skeletal muscle fibre; b, nerve terminal only; c, nerve terminal and terminal Schwann cell; d, nerve terminal, Schwann cell and two NMJ-capping cells; e, nerve terminal and two NMJ-capping cells; f, two NMJ-capping cells; g/h, the two NMJ-capping cells shown in isolation; i, orthogonal view of the reconstructed NMJ-capping cells. Animations of the volume rendering of these two cells are presented in supplementary material Movies 6 and 7. The NMJ-capping cells cover approximately 60% of the nerve terminal at this NMJ. In contrast to the terminal Schwann cell, the veil-like processes of both NMJ-capping cells extend beyond the immediate boundaries of the endplate. (D) Transmission electron micrograph through a neuromuscular junction in the rat diaphragm. The motor nerve terminal and terminal Schwann cell are covered by a slender process from a putative NMJ-capping cell (arrows). A high resolution image is reproduced in supplementary material Fig. S3. Scale bar: 2.5 μm.

of reactive terminal Schwann cells (Hayworth et al., 2006; Kang et al., 2007). As expected, nestin was expressed only in muscle fibres at innervated neuromuscular junctions; terminal Schwann cells remained nestin-negative for at least 2 days after denervation (Fig. 5D). However, the images suggest that profusion of 2166-positive cells was evident in the denervated endplate regions of TS muscles within 1 day of intercostal nerve injury; and many of these cells appeared to have grown processes interconnecting NMJs (Fig. 5E; supplementary material Figs S1 and S4). This response was local to denervated endplates: innervated NMJs in the same partially denervated muscles were covered by NMJ-capping cells confined to the ACh receptor cluster region, as in unoperated muscles. Some of the reactive, nestin-positive Schwann cell processes that formed 1-3 days later became associated with the 2166-positive cell processes interconnecting motor endplates (Fig. 5F; supplementary material Fig. S5) (41 junctions observed with this association in four muscles). We were unable to apply immunocytochemistry to study the relationship between S100-positive Schwann cells and 2166-positive NMJ-capping cells in mice, because both the 2166 antibody and commercial S100 antibody were raised in rabbits (and are hence unresolvable with anti-rabbit secondary antibodies). However, reactive Schwann cells in a partially denervated rat fourth deep lumbrical muscle stained using a mouse S100 antibody showed Schwann cell sprouts aligned with inter-endplate processes from 2166-positive NMJ-capping cells (supplementary material Figs S1B and S4).

The above findings suggested two hypotheses: first, that NMJ-capping cells selectively proliferate after nerve injury and second,

that these cells play an instructive role in sprouting by first activating terminal Schwann cells and then guiding their sprouts to denervated endplates. The data below support the first hypothesis but not the second, suggesting that the NMJ-capping cell response to denervation, paralysis or muscle atrophy probably occurs independently of the terminal Schwann cell reaction.

To test the first hypothesis we denervated TS muscles of seven adult mice and injected them with bromodeoxyuridine (BrdU) either 1 day (three mice) or 3 days (four mice) later. Incorporation of BrdU by NMJ-capping cells was assessed by immunofluorescence. Nuclei of NMJ-capping cells were distinguished from others (muscle and Schwann cell nuclei) by the characteristic 2166 staining forming lasso-like structures around the nuclei (see also Fig. 1, for example). We expected that the BrdU pulse would only mark cells within the first hour of injection, thus labelling only a small fraction of the 2166-positive cells that have proliferated. We were therefore not surprised by the apparent absence of BrdU labelling at 1 day; and by 3 days, only about 7% of all 2166-positive cells were BrdU positive. However, more than 65% of these cells were located within 40 μm of the neuromuscular junctions (Fig. 5G). These observations suggest that NMJ-capping cells were stimulated to spread, then divide, as an early consequence of endplate denervation. However, from these data we cannot exclude the possibility that the 2166-positive cells in the denervated endplate region become supplemented by invasion of reactive cells from outside the endplate zone as well.

To resolve whether the spread and proliferation of NMJ-capping cells could constitute an instructive signal that triggers the Schwann cell reaction to denervation (Son et al., 1996), we took advantage
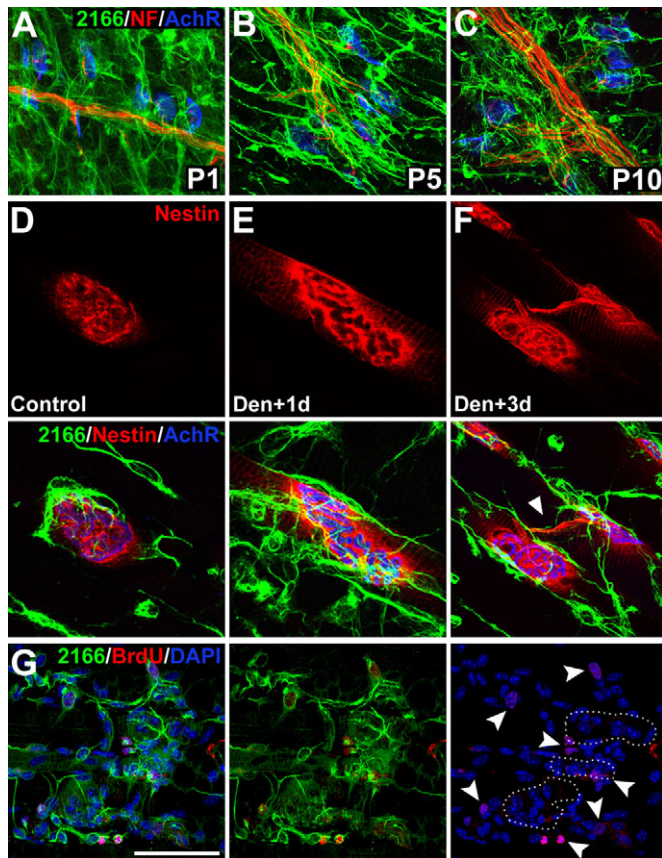
Fig. 5. NMJ-capping cells become restricted to the endplate zone postnatally but spread following denervation in adults. (A-C) 2166 immunostaining (green) is diffuse at birth but becomes progressively concentrated near NMJs over the following 1-2 weeks. (D-F) Denervation in adults triggers nestin reactivity and sprouting in terminal Schwann cells within 3 days but no discernible sprouting or nestin immunoreactivity is seen 1 day after axotomy. By contrast, extensive spreading of 2166 immunostaining occurs within 1 day of axotomy (see also supplementary material Fig. S4). At 3 days, some of the Schwann cell sprouts were associated with 2166-positive links between motor endplates (arrowhead) (see also supplementary material Fig. S5). (G) Immunostaining following injection of a BrdU pulse shows BrdU positive staining (red) of nuclei (blue) in both junctional and non-junctional 2166-positive cells (green), suggesting that NMJ-capping cells both divide and spread from endplates following axotomy. Arrowheads indicate BrdU-positive nuclei. Dotted lines indicate the location of three motor endplates, visualized by Alexa-Fluor-647-conjugated α-bungarotoxin (not shown). Scale bar: 100 μm (A-C); 50 μm (D-G).

discernible evidence of sprouting for at least 6 days (Fig. 6A-B). The 2166-positive cells were clearly dispersed over and between neuromuscular junctions, as in denervated muscle (compare with Fig. 5). Since the Schwann cell and NMJ-capping cell reactions were dissociated in time by BoNT/A paralysis, we conclude that the role of NMJ-capping cells in adaptive responses to nerve injury might be to lay down a substrate that could promote reactive Schwann cell outgrowth, but this does not necessarily trigger or instruct terminal Schwann cells to react. These cells evidently respond to cues arising from denervated or paralysed muscles independently of those that trigger earlier reaction of NMJ-capping cells.

Since denervation and paralysis had distinct temporal effects on terminal Schwann cells in TS muscles, but both were sufficient to induce NMJ-capping cell proliferation and spread, we next asked whether inactivity was strictly necessary for this reaction or whether some other, intrinsic signal from muscle fibres was sufficient. To test this we examined NMJ-capping cells in TS muscles of R6/2 transgenic mice, which are normally used to model Huntington's disease (Mangiarini et al., 1996). These mice develop profound, constitutive muscle atrophy and show several other characteristics of denervated muscle, even though their muscle fibres are fully innervated and they show no physiological evidence of paralysis. In fact, there are very few discernible abnormalities in the morphology of either Schwann cells or motor nerve terminals at most (>95%) of the NMJs in these mice (Ribchester et al., 2004). Muscle atrophy in R6/2 mice is therefore likely to be either myogenic or to have some other non-neural explanation. Moreover,
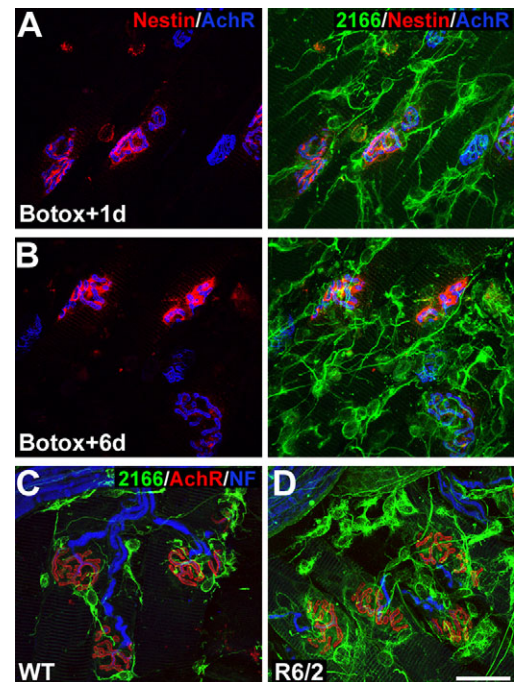

Fig. 6. NMJ-capping cells also spread in paralysed and atrophic muscles. (A,B) Profusion of 2166 immunoreactivity (green) is seen within 1 day of injection of a locally paralysing dose of botulinum toxin type-A (Botox) but terminal Schwann-cell reactivity and sprouting, assessed by nestin immunostaining (red), is not observed until after least 6 days of paralysis in TS muscles. (C,D) Similar profusion and spread of NMJ-capping cells is observed in constitutively atrophic muscles of 15-week-old R6/2 transgenic mice. Littermate controls show normal, endplate-localised staining and distribution of NMJ-capping cells. Scale bar: 50 μm.

of the slow response of Schwann cells and axons in the TS muscle to neuromuscular paralysis (unpublished observations), similar to that reported for 'fasyn' types of muscle by Pun et al. (Pun et al., 2002). We injected botulinum toxin type A (BoNT/A) into the interstitial spaces between the TS and intercostal muscles. The animals were sacrificed 1-6 days later. Stimulation of the intercostal nerves supplying the isolated muscles gave no contractile response, confirming the neuromuscular block, whereas stimulation of saline-injected control muscles produced vigorous muscle contractions.

The responses of NMJ-capping cells and terminal Schwann cells in BoNT/A-injected muscles were quite different from those in denervated muscle. After only 1 day of muscle paralysis, the profusion of 2166-positive cells in the junctional region was not discernibly different from that induced by denervation. However, terminal Schwann cells remained nestin negative and failed to show

Schwann cells and axons retain their capacity to sprout when muscles in R6/2 mice are surgically denervated, similarly to normal mice (Ribchester et al., 2004). We therefore used 2166 antibody to immunostain TS muscles dissected from two 15-week-old R6/2 mice, towards the end stage of disease. As expected (Carter et al., 1999), both of these mice showed decreased body weight and major muscle atrophy. If denervation or paralysis were necessary for the NMJ-capping cell reaction, we would have expected to see no difference in their distribution in R6/2 mouse muscles compared with wild-type mice, in spite of their muscle atrophy.

Surprisingly, the appearance and disposition of 2166-positive cells in R6/2 mice were similar to that observed following either denervation or paralysis of wild-type muscle (Fig. 6C,D). These observations support the interpretation that activation of NMJ-capping cells does not inevitably or invariably lead to activation of Schwann cells. The data also suggest that denervation and paralysis, although sufficient (see above), are not necessary for the induction of the NMJ-capping proliferation and spread. Thus, taken together, the NMJ-capping cell reaction that evidently occurred in all three circumstances – denervation, paralysis and atrophy (without paralysis) – suggests that factors triggering or triggered by atrophy of muscle fibres are responsible for their reactivity, rather than factors associated directly with reactive terminal Schwann cells.

What molecules cue the NMJ-capping cell reaction?
Previous data suggest that reactive perisynaptic fibroblasts express several adhesion molecules including tenascin-C, N-CAM, fibronectin and heparan sulphate proteoglycan and that perisynaptic fibroblasts might be one source of tenascin-C (Covault and Sanes, 1985; Sanes et al., 1986; Gatchalian et al., 1989; Weis et al., 1991). These molecules have also been implicated in nerve sprouting and regeneration (Cifuentes-Diaz et al., 2002). Confirming this, we observed no positive immunostaining for tenascin-C in innervated neuromuscular synapses of wild-type mice but strong immunostaining for this molecule at neuromuscular junctions denervated for 3 days (Fig. 7A,B). After 6 days, tenascin-C expression had also spread from the neuromuscular perimeter and 2166-positive cells were located in these tenascin-C-immunopositive regions (Fig. 7C).

Next, we examined the pattern of tenascin-C immunostaining following TS muscle denervation in tenascin-C-null mutant mice. We carried out X-gal staining of denervated muscles in a group of heterozygous tenascin-C-null mice in which the deleted sequence was substituted with a *lacZ* reporter gene (Saga et al., 1992; Garcion et al., 2004). As expected, we found no positive β-gal staining in innervated regions of TS muscles from these mice. However, 5 days after nerve section, there was strong positive staining of the intramuscular axon and motor endplate region only: areas expected to comprise Schwann cells or endoneurial or perineurial fibroblasts, and also consistent with tenascin-C expression by NMJ-capping cells (Fig. 7D,E). However, there was no compelling evidence that other 2166-positive cells expressed tenascin-C (compare Fig. 7C with Fig. 7D,E). Finally, we immunostained TS muscles with 2166 antibody in four homozygous tenascin-C-null mice before and after intercostal nerve section. In unoperated muscles, NMJ-capping cellular localisation was indistinguishable from wild-type controls, suggesting that tenascin-C is not necessary for accumulation of these cells to NMJs during postnatal development (compare Fig. 7F with Fig. 1A-D and Fig. 5E,F). There was no discernible difference in the NMJ-capping reaction within the first 48 hours of denervation either (Fig. 7G).

We therefore conclude that expression of tenascin-C, although normally associated with the spread of NMJ-capping cells following denervation, is neither required for the initial localisation of NMJ-capping cells to endplates during development, nor for their proliferation and spread following nerve injury. Presumably, other molecules, or combinations of molecules, mediate the NMJ-capping cell reaction.
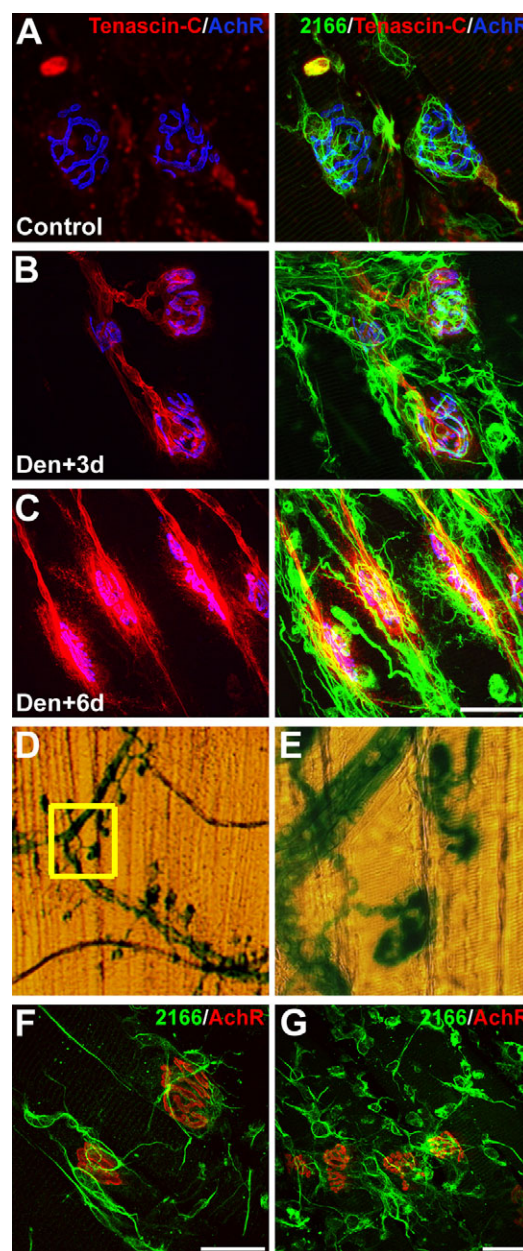

Fig. 7. Reactive NMJ-capping cells are associated with tenascin-C expression but do not require tenascin-C in order to localise, react or spread from NMJs. (A-C) Tenascin-C immunoreactivity (red) spread from the endplate region from 3-6 days after axotomy (left panels) and these tenascin-C-rich regions coincide with the distribution of NMJ-capping cells (green, right panels; AChR counterstained blue). (D,E) Selective X-Gal staining of intramuscular nerve and motor endplates in heterozygous tenascin-C-null mutant mice with *lacZ* substitution, 5 days after axotomy. The area shown in E corresponds to the area bounded by the boxed outline in D. Unoperated muscles were X-Gal negative (not shown). (F,G) NMJ-capping cells are also localised to NMJ in homozygous tenascin-C-null mutant mice and these cells spread from endplates 3 days after axotomy, as in wild-type mice. Scale bar in C, right: 50 μm (A-C), 100 μm (D), 30 μm (E). Scale bars in F and G: 50 μm.

Discussion

The results suggest that mammalian NMJs normally comprise four cell types: muscle fibre, motor neuron, terminal Schwann cell and the NMJ-capping cell (a neglected cell-type that merits further investigation as a potential moderator of neuromuscular synaptic development, maintenance and plasticity). Evidence for this is summarised below, where we also discuss in more detail, the identity of NMJ-capping cells, the possible significance of their immunocytochemical profile and their development and plasticity.

First, serendipitously, we found that antibody 2166 immunostains a distinct population of cells capping NMJs, lying outside the synaptic basal lamina but colocalising with terminal Schwann cells, motor nerve terminals and muscle fibres at motor endplates. Confocal microscopy of whole mounts immunostained with the 2166 antibody and other markers were pivotal in demonstrating the consistent presence and association of NMJ-capping cells with motor endplates. It is perhaps important to note that estimates of the numbers of terminal Schwann cells at motor endplates should therefore take into account the evidence that most NMJs also contain one to two NMJ-capping cells (see data in Fig. 1).

Second, NMJ-capping cells become restricted to the endplate region during postnatal development but react to either denervation or paralysis in adults by proliferation and spread from endplates. This occurs more rapidly than the reactive response of terminal Schwann cells. NMJ-capping cells also take the lead in forming bridges (or consolidating existing ones; see Fig. 3) between neuromuscular junctions following muscle denervation or paralysis, ahead of terminal Schwann cells. This finding might be significant for understanding mechanisms of compensatory nerve sprouting and regeneration. NMJ-capping cells are also dispersed from NMJs in a disease model (R6/2 transgenic mice), where there is muscle atrophy but no paralysis or denervation. Since the structure and function of motor nerve terminals and terminal Schwann cells appear largely normal in these mice, a parsimonious explanation is that the signalling mechanism that induces the proliferation and spread of NMJ-capping cells derives from denervated, paralysed or atrophic muscle fibres rather than any other cell type at NMJ.

Third, although the above suggest that one of the functions of NMJ-capping cells is to repair damaged neuromuscular connections, the data also suggest that the NMJ-capping cell reaction does not require or depend on tenascin-C, an early molecular marker previously associated with axonal sprouting and regeneration.

The identity of NMJ-capping cells

The present data underscore the importance of a pioneering ultrastructural study by Robertson (Robertson, 1956) who identified 'endothelial' cells associated with the NMJ. The consistency of this association and the potential role of these cells in maintenance of the normal structure and function of the NMJ has been somewhat neglected ever since. However, similar non-neural cells were identified in scanning electron micrographs by Desaki and Uehara (Desaki and Uehara, 1981), who described them as 'flattened stellate cells of unknown nature'. Other investigators recognised the association of fibroblast-like cells to NMJs (Murray and Robbins, 1982; Connor and McMahan, 1987; Connor, 1997; Caroni and Schneider, 1994) in their description of 'perisynaptic fibroblasts' (Covault and Sanes, 1985; Sanes et al., 1986; Connor and McMahan, 1987; Connor, 1997; Gatchalian et al., 1989; Weis et al., 1991). Perhaps perisynaptic fibroblasts and NMJ-capping cells are the same as the endothelial cells of Robertson (Robertson, 1956), but this remains unproven. Nevertheless, the parallels are striking: like

'perisynaptic fibroblasts' the capping cells proliferate in response to denervation; they are fibroblast-like; and they appear to change their gene expression in response to nerve injury. It is therefore rather surprising that reviewers have been reluctant to depict these cell types as essential components of the NMJ (Sanes and Lichtman, 1999; Hughes et al., 2006).

Taking the present and previous observations together, we suggest that the NMJ-capping cells ought now to be considered an integral cellular component of neuromuscular junctions and therefore represented as such in diagrammatic depictions of the neuromuscular junction (e.g. Fig. 8A). We propose naming these capping cells descriptively, as neuromuscular 'kranocytes' (from the Greek κρανος , which means helmet), which acknowledges their main morphological characteristic. We use this nomenclature for the remainder of the present discussion.

Immunocytochemical profile of kranocytes

We screened kranocytes using a panel of antibodies, including those previously associated with different cell types in skeletal muscle. Of the antibodies tested, HM-24, rPH and CD34 gave positive staining. Kranocytes also bound fluorescent CTB. The CD34 and CTB labels suggest a more complete covering of the NMJ by the capping cells than revealed by 2166 (or HM-24) staining. The explanation appears to be that 2166 stains the non-uniform
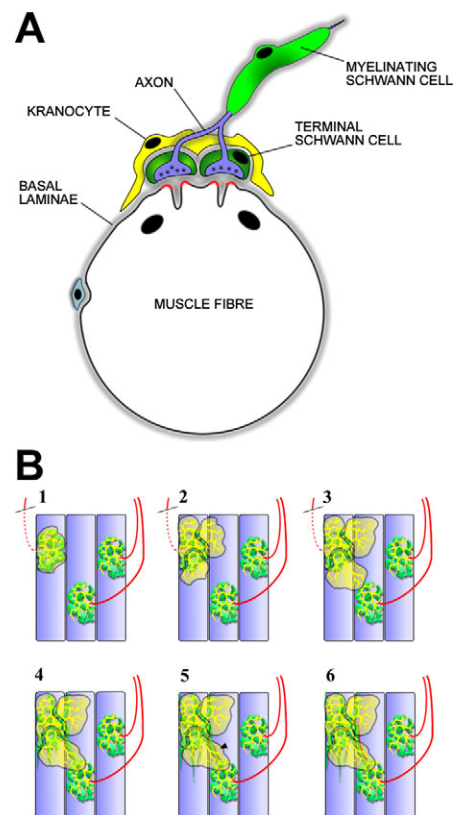
Fig. 8. NMJ-capping cells are integral, plastic cellular components of the NMJ. (A) Relationship between four main cell types proposed to constitute the mammalian NMJ: muscle fibre, motor nerve terminal, terminal (perisynaptic) Schwann cell and NMJ-capping cells, named here 'kranocytes' (see Discussion). (B) Stages in kranocyte reactivity to denervation, paralysis or muscle atrophy that could indicate a permissive function for these cells in terminal Schwann cell and axonal sprouting. Kranocyte sprouting is the first reaction, followed by terminal Schwann cell sprouting, then axonal sprouting.

distribution of a cytoskeletal protein, whereas CD34 antibody and CTB label the plasma membranes of these cells.

Staining with HM-24 antibody revealed an intriguing contrast to a previous study of the localisation of the antigen to NMJs. Trinidad et al. (Trinidad et al., 2000) reported HM-24 (neuregulin) immunoreactivity to be within terminal Schwann cells. However, our observations based on immunostaining in S100-GFP-expressing transgenics (see Fig. 2), suggest that kranocytes are HM-24 positive but terminal Schwann cells are not. The methods we used differ, principally in our use of triangularis sterni muscle whole-mounts rather than tissue sections. But since Trinidad et al. (Trinidad et al., 2000) did not appear to consider or rule out the possibility that HM-24 antibody might have immunostained a fourth cell type, we suggest their conclusion might have been mistaken. The localisation of neuregulin (or a neuregulin-like molecule) to kranocytes rather than terminal Schwann cells could have important implications for understanding the development and maintenance of neuromuscular junctions, so it will be important to resolve this issue.

The enzyme rPH is involved in the synthesis of collagen (Pihlajaniemi et al., 1991), but cell types other than fibroblasts, including endothelial cells and myelin-forming Schwann cells, also express rPH (Singh et al., 1997; Vanderwinden et al., 1999). Kranocytes were also immunopositive for CD34 antigen, previously identified as an endothelial or hematopoietic stem cell marker (Krause et al., 1994). CD34-positive and rPH-positive haematopoietic stem cells could give rise to fibroblasts (Lee et al., 2000; Zulli et al., 2005). It might therefore be interesting to investigate further the pluripotential (i.e. stem-cell) capacity of neuromuscular kranocytes, especially in light of a recent report suggesting that fibroblasts are reprogrammed into a fully pluripotential state following ectopic expression (via retroviral vectors) of the transcription factors Oct-4, Sox-2, Myc and Klf4 (Wernig et al., 2007; Takahashi et al., 2007).

The surface expression of the CTB receptor (a GM1 ganglioside) suggests another way that more information might be obtained about the normal functions of these cells. For instance, ablation of terminal Schwann cell at the neuromuscular junction can provide information about their short- and long-term functions in sustaining motor nerve terminals (Reddy et al., 2003; Halstead et al., 2004; Halstead et al., 2005). In preliminary experiments, we found that the antiganglioside antibody DG2 ablates motor nerve terminals, terminal Schwann cell and NMJ-capping cells by complement-mediated cell lysis (unpublished observations). If a more selective ablation of kranocytes becomes possible, it will be interesting to examine the long-term effects of this on neuromuscular development, maintenance and repair.

Developmental and plasticity of kranocytes

Cells positive for 2166 become restricted to the neuromuscular contact zone during postnatal development. A similar developmental restriction of non-neural cells to NMJs was reported in frogs (Connor, 1997). Whether this is due to changes in the composition of the basal lamina at the neuromuscular junction (Patton et al., 1998; Sanes et al., 1990; Cho et al., 1998) or other phenomena at endplates, such as endogenous electric fields (Betz et al., 1980; Kinnamon et al., 1985), remains to be established. Abnormalities of synaptic structure have been demonstrated in mutant mice that lack specific components of the synaptic basal lamina (Noakes et al., 1995; VanSaun et al., 2003). It will be interesting to examine the disposition of kranocytes in mutant mice lacking specific basal lamina components (or endogenous electric fields).

A role for kranocytes in neuromuscular plasticity is suggested by their reaction in adults to nerve injury or paralysis. This reaction occurred at least 2 days earlier than the reactive transformation of terminal Schwann cells. This early reaction does not detract from the pivotal role played by reactive terminal Schwann cells in leading regenerating axons to denervated or paralysed motor endplates (Son et al., 1996; Love and Thompson, 1998; Love and Thompson, 1999; Love et al., 2003; Kang et al., 2003). Rather, the data underscore the importance of terminal Schwann cells, by demonstrating that their transformation to a reactive state is not an inevitable consequence of early reaction and spread of kranocytes. Perhaps kranocytes consolidate the cellular bridges they appear to form between motor endplates, and these are subsequently utilised by reactive terminal Schwann cells. Terminal Schwann cell bridges then support subsequent axonal sprouting and regeneration (Fig. 8B). It is noteworthy that electrical stimulation of denervated rat muscle does not prevent Schwann cells from becoming reactive, but it strongly inhibits the formation of Schwann cell bridges between endplates (Love et al., 2003). It would be interesting to know whether stimulation also prevents the reaction of neuromuscular kranocytes to denervation.

We also found evidence of dispersal of the population of 2166-positive cells in atrophic muscles of the R6/2 transgenic mouse model of Huntington's disease. However, since motor nerve terminals, terminal Schwann cells and neuromuscular transmission appear largely normal in R6/2 mice (Ribchester et al., 2004), denervation, paralysis or muscle atrophy would appear to be sufficient to provoke the kranocyte cell reaction; but the reaction of these cells is evidently not sufficient to trigger the subsequent Schwann cell reaction in this disease model. It would be interesting to know the disposition and fate of kranocytes in other models of neuromuscular disease, particularly models of amyotrophic lateral sclerosis, where neuromuscular synaptic degeneration is among the earliest signs of disease (Fischer et al., 2004; Schaefer et al., 2005; Pun et al., 2006; Suzuki et al., 2007).

The focal distribution of a specific subpopulation of 2166-positive cells to neuromuscular junctions together with their progressive restriction to these areas during postnatal development and their persistence at synapses following muscle denervation, paralysis or atrophy, suggest important roles for kranocytes in the development, neurotrophic maintenance and repair of neuromuscular junctions. Several important questions remain: the possible gliotrophic function of kranocytes; the mechanism of their restriction to motor endplates and the function of this developmental restriction; the significance of their proliferation and spread in atrophic muscle; and finally, the identity of the 2166 antigen that was crucial in identifying these cells. Since we now have a very good marker for kranocytes, there is a much greater potential than in the past for obtaining more information about the functions of these intriguing cells. Harnessing the molecular secretions of these plastic cells could perhaps also be utilised in targeting potential neuroprotective factors to neuromuscular junctions, potentially mitigating or preventing early signs of neuromuscular disease.

Materials and Methods
Generation of 2166 antibody

The 2166 antibody was generated from a peptide (amino acid sequence CAIRNSRDVI) corresponding to the C-terminus of the Tspan-2 protein, coupled to keyhole limpet hemocyanin (KLH). This peptide was used to inoculate male New Zealand white rabbits of approximately 1.5 kg in weight. After three injections of KLH-coupled peptide, serum was collected at appropriate time points and affinity purified. We made a preliminary attempt to identify the putative antigen by western blotting of a cytoskeletal protein fraction from cerebellum (data not shown). The antibody recognised a band of approximately 47 kDa. Analysis by mass spectrometry was consistent with an antigen of similar molecular weight to tubulin. Pre-immune

serum was inactive and specific staining was blocked by preincubating the active serum with the peptide used to raise the antibody. However, we were unable to achieve immunoprecipitation of any specific protein with the 2166 antibody and it did not recognise purified tubulin on western blots. A more stringent fractionation and/or proteomic analysis is therefore necessary to identify the 2166 antigen.

Animals and surgery

All animals were maintained in a regulated, clean environment and treated in compliance with UK Home Office regulations. Adult female Sprague-Dawley rats were used in some experiments but most were performed using the following mouse lines: C57Bl/6, S100-eGFP transgenic (accessed during a visit to Pico Caroni's laboratory), R6/2 transgenic (Ribchester et al., 2004) and tenascin-C-null mutant (TNC/TN-F18) (Saga et al., 1992) (a gift from Charles ffrench-Constant, Dept of Pathology, University of Cambridge, UK). Tenascin-C-null mutant mice were genotyped as described (Garcion et al., 2004). In some experiments, adult mice were anaesthetised intraperitoneally with 1 mg/kg medetomidine (Domitor), 75 mg/kg ketamine (Vetalar) and one or more of the intercostal nerves supplying the triangularis sterni (TS) muscle were crushed unilaterally. In other anaesthetised adult mice, intercostal muscles adjacent to the TS muscle were injected with 2.5 μl botulinum toxin type A (BoNT/A;10 ng/ml; Sigma) from a Hamilton syringe. Surgically prepared animals were allowed to recover for 1-6 days. All animals were killed by cervical dislocation.

Immunocytochemistry and histochemistry

Whole-mount preparations were made by dissecting TS muscles in 0.1 M phosphate-buffered saline (PBS, pH 7.4), fixed in 4% paraformaldehyde for 20 minutes, then incubated in either TRITC- or Alexa Fluor 647 conjugates of α-bungarotoxin (Molecular Probes; 5 μg/ml for 30 minutes). After washing in PBS and blocking/permeabilisation for 1 hour in 1% BSA, 0.4% lysine, 0.5% Triton X-100 in PBS, primary antibodies (see below) were applied overnight at 4°C. Muscles were washed and incubated with secondary antibodies for 3.5 hours at room temperature, washed and mounted in Vectashield (Vector Labs). Most of the observations reported were based on analysis of four whole-mount preparations per immunostain combination. For muscle section immunocytochemistry, dissected muscles were embedded in OCT (Tissue TEK) and frozen in isopentane precooled with liquid nitrogen. Cryostat sections were collected, fixed with 4% paraformaldehyde for 5 minutes, then blocked and permeabilised for 1 hour with 5% fish gelatine and 0.1% Triton X-100 in PBS. Primary antibodies (see below) were applied overnight at room temperature. Sections were washed and incubated with secondary antibodies for 1 hour at room temperature, washed in PBS and mounted in Vectashield. Preparations were viewed using a Bio-Rad Radiance 2000 confocal microscope on a Nikon Eclipse E600-FN platform. For staining with cholera toxin B (CTB), TS muscles from male Balb/c mice (6-8 weeks) were dissected, pinned on Sylgard-lined dishes and bathed in FITC-conjugated CTB (Sigma, 1:300) and a Texas-Red conjugate of α-bungarotoxin (Molecular Probes, Eugene), diluted 1:500 in oxygenated saline for 2 hours at 32°C, followed by 30 minutes at 4°C, rinsed in buffer, fixed at room temperature for 15 minutes in 4% paraformaldehyde, rinsed in 0.1 M glycine and mounted in Citifluor anti-fade reagent (Citifluor, Canterbury, UK). Images were obtained using a Zeiss Pascal confocal microscope. Voxx rendering software (Clendenon et al., 2002) was used for 3D reconstruction. *LacZ* expression in whole mounts of TS muscles from heterozygous tenascin-C-null mutant mice was detected by X-gal staining solution, with a solution containing 2 mM MgCl$_2$, 5 mM K$_3$Fe(CN)$_6$, 5 mM 0.02% NP-40 and 1 mg/ml X-gal (5-bromo-4-chloro-3-indolyl-D-galactoside; Sigma). Image post-processing was carried out using Adobe Photoshop and/or Image J software.

Source and dilution of species-specific antibodies

Antibodies were obtained from the following suppliers and used at indicated dilutions: rabbit 2166 (Peter Brophy, University of Edinburgh; 1:200); mouse anti-desmin (DAKO; 1:200); rat IgG2k F4/80 (Serotec; 1:50); mouse IgG1 anti-GFAP (Boehringer; 1:100); rat IgG anti-Laminin (a2 chain) (Alexis; 1:200); rabbit anti-M-Cadherin (Anton Wernig, University of Bonn; 1:50); rabbit anti-N-CAM (Elisabeth Bock, University of Copenhagen; 1:100); mouse IgG1 anti-Nestin (Susan Hockfield, Yale University; 1:200); mouse anti-neurofilament (165 kDa) (DHSB; 1:200); rabbit anti-S100 (DAKO; 1:200); mouse IgG1 anti-S100 (SA1259) (Affinity; 1:200); mouse anti-SV2 (SAPU; 1:200); mouse IgG1 anti-Thy 1.1 (Serotec; 1:100); rat IgG2b anti-CD34 (BD PharMingen; 1:50); mouse IgG1 anti-prolyl-4-hydroxylase (Acris Medicorp; 1:100); rat IgG anti-tenascin (Abcam; 1:200); rabbit HM-24 (Jonathan Cohen, Harvard Medical School; 1:200).

Electron microscopy

Isolated mouse TS muscle was fixed in 4% paraformaldehyde and 2.5% glutaraldehyde in ice-cold 0.1 M phosphate buffer for 4 hours, then post-fixed in 1% osmium tetroxide for 45 minutes, dehydrated in ethanol and propylene oxide and embedded in Durcupan resin. 300 ultrathin (75-100 nm) serial sections were cut from the endplate region, collected on formvar-coated grids (Agar Scientific), stained with uranyl acetate and lead citrate then viewed in a Philips CM12 transmission electron microscope. Electron photomicrograph negatives were scanned at 1000 dpi. A few sections were lost during preparation (<20 out of 300), so these were replaced in the final image stack by a duplicate of a neighbouring serial section. Digitised micrographs were then transferred

to a Unix workstation (Sun Microsystems) and a custom program (Reconstruct) was used to generate 3D-voxel images. The program 'MAPaint' was used to reconstruct 3D volumes of the nerve terminal, skeletal muscle fibre, terminal Schwann cell and 2166-positive cells. Both Reconstruct and MAPaint were written and developed in the MRC Human Genetics Unit, Edinburgh http://genex.hgu.mrc.ac.uk). Different cell types were identified in each individual 2D image before manually delineating their borders. The 3D volumes were saved to independent files, calibrated and surface rendered using Imaris software (Bitplane; Zurich, Switzerland).

References

Aiba, S., Tabata, N., Ohtani, H. and Tagami, H. (1994). CD34+ spindle-shaped cells selectively disappear from the skin lesion of scleroderma. *Arch. Dermatol.* **130**, 593-597.

Austyn, J. M. and Gordon, S. (1981). F4/80: a monoclonal antibody directed specifically against the mouse macrophage. *Eur. J. Immunol.* **11**, 805-815.

Barry, J. A. and Ribchester, R. R. (1995). Persistent polyneuronal innervation in partially denervated rat muscle after reinnervation and recovery from prolonged nerve conduction block. *J. Neurosci.* **15**, 6327-6339.

Beeson, D., Higuchi, O., Palace, J., Cossins, J., Spearman, H., Maxwell, S., Newsom-Davis, J., Burke, G., Fawcett, P., Motomura, M. et al. (2006). Dok-7 mutations underlie a neuromuscular junction synaptopathy. *Science* **313**, 1975-1978.

Betz, W. J., Caldwell, J. H., Ribchester, R. R., Robinson, K. R. and Stump, R. F. (1980). Endogenous electric field around muscle fibres depends on the Na+-K+ pump. *Nature* **287**, 235-237.

Birks, R., Huxley, H. E. and Katz, B. (1960). The fine structure of the neuromuscular junction of the frog. *J. Physiol.* **150**, 134-144.

Birling, M. C., Tait, S., Hardy, R. J. and Brophy, P. J. (1999). A novel rat tetraspan protein in cells of the oligodendrocyte lineage. *J. Neurochem.* **73**, 2600-2608.

Brown, M. C. and Ironton, R. (1978). Sprouting and regression of neuromuscular synapses in partially denervated mammalian muscles. *J. Physiol.* **278**, 325-348.

Brown, M. C., Holland, R. L. and Ironton, R. (1980). Nodal and terminal sprouting from motor nerves in fast and slow muscles of the mouse. *J. Physiol.* **306**, 493-510.

Caroni, P. and Schneider, C. (1994). Signaling by insulin-like growth factors in paralyzed skeletal muscle, rapid induction of IGF1 expression in muscle fibres and prevention of interstitial cell proliferation by IGF-BP5 and IGF-BP4. *J. Neurosci.* **14**, 3378-3388.

Carter, R. J., Lione, L. A., Hunt, M. J., Humby, T., Mangiarini, L., Mahal, A., Bates, G. P., Dunnett, S. B. and Morton, A. J. (1999). Characterisation of progressive motor deficits in mice transgenic for the human Huntington's Disease mutation. *J. Neurosci.* **19**, 3248-3257.

Castonguay, A. and Robitaille, R. (2001). Differential regulation of transmitter release by presynaptic and glial Ca2+ internal stores at the neuromuscular synapse. *J. Neurosci.* **21**, 1911-1922.

Cho, S. I., Ko, J., Patton, B. L., Sanes, J. R. and Chiu, A. Y. (1998). Motor neurons and Schwann cells distinguish between synaptic and extrasynaptic isoforms of laminin. *J. Neurobiol.* **37**, 339-358.

Cifuentes-Diaz, C., Faille, L., Goudou, D., Schachner, M., Rieger, F. and Angaut-Petit, D. (2002). Abnormal reinnervation of skeletal muscle in a tenascin-C-deficient mouse. *J. Neurosci. Res.* **67**, 93-99.

Clendenon, J. L., Phillips, C. L., Sandoval, R. M., Fang, S. and Dunn, K. W. (2002). Voxx: a PC-based, near real-time volume rendering system for biological microscopy. *Am. J. Physiol., Cell Physiol.* **282**, C213-C218.

Connor, E. A. (1997). Developmental regulation of interstitial cell density in bullfrog skeletal muscle. *J. Neurocytol.* **26**, 23-32.

Connor, E. A. and McMahan, U. J. (1987). Cell accumulation in the junctional region of denervated muscle. *J. Cell Biol.* **104**, 109-120.

Costanzo, E. M., Barry, J. A. and Ribchester, R. R. (1999). Co-regulation of synaptic efficacy at stable polyneuronally innervated neuromuscular junctions in reinnervated rat muscle. *J. Physiol.* **521**, 365-374.

Costanzo, E. M., Barry, J. A. and Ribchester, R. R. (2000). Competition at silent synapses in reinnervated skeletal muscle. *Nat. Neurosci.* **3**, 694-700.

Court, F. A., Sherman, D. L., Pratt, T., Garry, E. M., Ribchester, R. R., Cottrell, D. F., Fleetwood-Walker, S. M. and Brophy, P. J. (2004). Restricted growth of Schwann cells lacking Cajal bands slows conduction in myelinated nerves. *Nature* **431**, 191-195.

Court, F. A., Brophy, P. J. and Ribchester, R. R. (2008). Remodeling of motor nerve terminals in demyelinated axons of periaxin-null mice. *Glia.* **56**, 471-479.

Covault, J. and Sanes, J. R. (1985). Neural cell adhesion molecule (N-CAM) accumulates in denervated and paralyzed skeletal muscles. *Proc. Natl. Acad. Sci. USA* **82**, 4544-4548.

David, G., Nguyen, K. and Barrett, E. F. (2007). Early vulnerability to ischemia/reperfusion injury in motor terminals innervating fast muscles of SOD1-G93A mice. *Exp. Neurol.* **204**, 411-420.

Desaki, J. and Uehara. Y. (1981). The overall morphology of neuromuscular junctions as revealed by scanning electron microscopy. *J. Neurocytol.* **10**, 101-110.

Feng, G., Laskowski, M. B., Feldheim, D. A., Wang, H., Lewis, R., Frisen, J., Flanagan, J. G. and Sanes, J. R. (2000). Roles for ephrins in positionally selective synaptogenesis between motor neurons and muscle fibres. *Neuron* **25**, 295-306.

Fischer, L. R., Culver, D. G., Tennant, P., Davis, A. A., Wang, M., Castellano-Sanchez, A., Khan, J., Polak, M. A. and Glass, J. D. (2004). Amyotrophic lateral sclerosis is a distal axonopathy: evidence in mice and man. *Exp. Neurol.* **185**, 232-240.

Fukada, S., Higuchi, S., Segawa, M., Koda, K., Yamamoto, Y., Tsujikawa, K., Kohama, Y., Uezumi, A., Imamura, M., Miyagoe-Suzuki, Y. et al. (2004). Purification and cell-surface marker characterization of quiescent satellite cells from murine skeletal muscle by a novel monoclonal antibody. *Exp. Cell Res.* **296**, 245-255.

Garcion, E., Halilagic, A., Faissner, A. and ffrench-Constant, C. (2004). Generation of an environmental niche for neural stem cell development by the extracellular matrix molecule tenascin C. *Development* **131**, 3423-3432.

Gatchalian, C. L., Schachner, M. and Sanes, J. R. (1989). Fibroblasts that proliferate near denervated synaptic sites in skeletal muscle synthesize the adhesive molecules tenascin(J1), N-CAM, fibronectin, and a heparan sulfate proteoglycan. *J. Cell Biol.* **108**, 1873-1890.

Halstead, S. K., O'Hanlon, G. M., Humphreys, P. D., Morrison, D. B., Morgan, B. P., Todd, A. J., Plomp, J. J. and Willison, H. J. (2004). Anti-disialoside antibodies kill perisynaptic Schwann cells and damage motor nerve terminals via membrane attack complex in a murine model of neuropathy. *Brain* **127**, 2109-2123.

Halstead, S. K., Morrison, I., O'Hanlon, G. M., Humphreys, P. D., Goodfellow, J. A., Plomp, J. J. and Willison, H. J. (2005). Anti-disialosyl antibodies mediate selective neuronal or Schwann cell injury at mouse neuromuscular junctions. *Glia* **52**, 177-189.

Hayworth, C. R., Moody, S. E., Chodosh, L. A., Krieg, P., Rimer, M. and Thompson, W. J. (2006). Induction of neuregulin signaling in mouse schwann cells in vivo mimics responses to denervation. *J. Neurosci.* **26**, 6873-6884.

Hudson, C. S., Deshpande, S. S. and Albuquerque, E. X. (1984). Consequences of axonal transport blockade by batrachotoxin on mammalian neuromuscular junction. III. An ultrastructural study. *Brain Res.* **296**, 319-332.

Hughes, B. W., Kusner, L. L. and Kaminski, H. J. (2006). Molecular architecture of the neuromuscular junction. *Muscle Nerve* **33**, 445-461.

Jahromi, B. S., Robitaille, R. and Charlton, M. P. (1992). Transmitter release increases intracellular calcium in perisynaptic Schwann cells in situ. *Neuron* **8**, 1069-1077.

Kang, H., Tian, L. and Thompson, W. (2003). Terminal Schwann cells guide the reinnervation of muscle after nerve injury. *J. Neurocytol.* **32**, 975-985.

Kang, H., Tian, L., Son, Y. J., Zuo, Y., Procaccino, D., Love, F., Hayworth, C., Trachtenberg, J., Mikesh, M., Sutton, L. et al. (2007). Regulation of the intermediate filament protein nestin at rodent neuromuscular junctions by innervation and activity. *J. Neurosci.* **27**, 5948-5957.

Kinnamon, S. C., Betz, W. J. and Caldwell, J. H. (1985). Development of a steady electric current in neonatal rat lumbrical muscle. *Dev. Biol.* **112**, 241-247.

Krause, D. S., Ito, T., Fackler, M. J., Smith, O. M., Collector, M. I., Sharkis, S. J. and May, W. S. (1994). Characterization of murine CD34, a marker for hematopoietic progenitor and stem cells. *Blood* **84**, 691-701.

Lee, J. Y., Qu-Petersen, Z., Cao, B., Kimura, S., Jankowski, R., Cummins, J., Usas, A., Gates, C., Robbins, P., Wernig, A. et al. (2000). Clonal isolation of muscle-derived cells capable of enhancing muscle regeneration and bone healing. *J. Cell Biol.* **150**, 1085-1100.

Love, F. M. and Thompson, W. J. (1998). Schwann cells proliferate at rat neuromuscular junctions during development and regeneration. *J. Neurosci.* **18**, 9376-9385.

Love, F. M. and Thompson, W. J. (1999). Glial cells promote muscle reinnervation by responding to activity-dependent postsynaptic signals. *J. Neurosci.* **19**, 10390-10396.

Love, F. M., Son, Y. J. and Thompson, W. J. (2003). Activity alters muscle reinnervation and terminal sprouting by reducing the number of Schwann cell pathways that grow to link synaptic sites. *J. Neurobiol.* **54**, 566-576.

Mangiarini, L., Sathasivam, K., Seller, M., Cozens, B., Harper, A., Hetherington, C., Lawton, M., Trottier, Y., Lehrach, H., Davies, S. W. et al. (1996). Exon 1 of the HD gene with an expanded CAG repeat is sufficient to cause a progressive neurological phenotype in transgenic mice. *Cell* **87**, 493-506.

Miledi, R. and Slater, C. R. (1970). On the degeneration of rat neuromuscular junctions after nerve section. *J. Physiol.* **207**, 507-528.

Murray, M. A. and Robbins, N. (1982). Cell proliferation in denervated muscle: time course, distribution and relation to disuse. *Neuroscience* **7**, 1817-1822.

Nissi, R., Autio-Harmainen, H., Marttila, P., Sormunen, R. and Kivirikko, K. I. (2001). Prolyl 4-hydroxylase isoenzymes I and II have different expression patterns in several human tissues. *J. Histochem. Cytochem.* **49**, 1143-1153.

Noakes, P. G., Gautam, M., Mudd, J., Sanes, J. R. and Merlie, J. P. (1995). Aberrant differentiation of neuromuscular junctions in mice lacking s-laminin/laminin beta 2. *Nature* **374**, 258-262.

Patton, B. L., Chiu, A. Y. and Sanes, J. R. (1998). Synaptic laminin prevents glial entry into the synaptic cleft. *Nature* **393**, 698-701.

Peters, A., Palay, S. L. and Webster, H. de F. (1991). *The Fine Structure of the Nervous System: Neurons and Their Supporting Cells*. 3rd Edn. Oxford: Oxford University Press.

Pihlajaniemi, T., Myllyla, R. and Kivirikko, K. I. (1991). Prolyl 4-hydroxylase and its role in collagen synthesis. *J. Hepatol.* **13 Suppl. 3**, S2-S7.

Pun, S., Sigrist, M., Santos, A. F., Ruegg, M. A., Sanes, J. R., Jessell, T. M., Arber, S. and Caroni, P. (2002). An intrinsic distinction in neuromuscular junction assembly and maintenance in different skeletal muscles. *Neuron* **34**, 357-370.

Pun, S., Santos, A. F., Saxena, S., Xu, L. and Caroni, P. (2006). Selective vulnerability and pruning of phasic motoneuron axons in motoneuron disease alleviated by CNTF. *Nat. Neurosci.* **9**, 408-419.

Reddy, L. V., Koirala, S., Sugiura, Y., Herrera, A. A. and Ko, C. P. (2003). Glial cells maintain synaptic structure and function and promote development of the neuromuscular junction *in vivo*. *Neuron* **40**, 563-580.

Reynolds, M. L. and Woolf, C. J. (1992). Terminal Schwann cells elaborate extensive processes following denervation of the motor endplate. *J. Neurocytol.* **21**, 50-66.

Ribchester, R. R., Thomson, D., Wood, N. I., Hinks, T., Gillingwater, T. H., Wishart, T. M., Court, F. A. and Morton, A. J. (2004). Progressive abnormalities in skeletal muscle and neuromuscular junctions of transgenic mice expressing the Huntington's disease mutation. *Eur. J. Neurosci.* **20**, 3092-3114.

Robertson, J. D. (1956). The ultrastructure of a reptilian myoneural junction. *J. Biophys. Biochem. Cytol.* **2**, 381-394.

Saga, Y., Yagi, T., Ikawa, Y., Sakakura, T. and Aizawa, S. (1992). Mice develop normally without tenascin. *Genes Dev.* **6**, 1821-1831.

Sanes, J. R. and Lichtman, J. W. (1999). Development of the vertebrate neuromuscular junction. *Annu. Rev. Neurosci.* **22**, 389-442.

Sanes, J. R., Schachner, M. and Covault, J. (1986). Expression of several adhesive macromolecules (N-CAM, L1, J1, NILE, uvomorulin, laminin, fibronectin, and a heparan sulfate proteoglycan) in embryonic, adult, and denervated adult skeletal muscle. *J. Cell Biol.* **102**, 420-431.

Sanes, J. R., Engvall, E., Butkowski, R. and Hunter, D. D. (1990). Molecular heterogeneity of basal laminae, isoforms of laminin and collagen IV at the neuromuscular junction and elsewhere. *J. Cell Biol.* **111**, 1685-1699.

Schaefer, A. M., Sanes, J. R. and Lichtman, J. W. (2005). A compensatory subpopulation of motor neurons in a mouse model of amyotrophic lateral sclerosis. *J. Comp. Neurol.* **490**, 209-219.

Singh, N., Birdi, T. J., Chandrashekar, S. and Antia, N. H. (1997). Schwann cell extracellular matrix protein production is modulated by Mycobacterium leprae and macrophage secretory products. *J. Neurol. Sci.* **151**, 13-22.

Slater, C. R., Lyons, P. R., Walls, T. J., Fawcett, P. R. and Young, C. (1992). Structure and function of neuromuscular junctions in the vastus lateralis of man. A motor point biopsy study of two groups of patients. *Brain* **115**, 451-478.

Smith, S. C., Folefac, V. A., Osei, D. K. and Revell, P. A. (1998). An immunocytochemical study of the distribution of proline-4-hydroxylase in normal, osteoarthritic and rheumatoid arthritic synovium at both the light and electron microscopic level. *Br. J. Rheumatol.* **37**, 287-291.

Son, Y. J. and Thompson, W. J. (1995). Schwann cell processes guide regeneration of peripheral axons. *Neuron* **14**, 125-132.

Son, Y. J., Trachtenberg, J. T. and Thompson, W. J. (1996). Schwann cells induce and guide sprouting and reinnervation of neuromuscular junctions. *Trends Neurosci.* **19**, 280-285.

Suzuki, M., McHugh, J., Tork, C., Shelley, B., Klein, S. M., Aebischer, P. and Svendsen, C. N. (2007). GDNF secreting human neural progenitor cells protect dying motor neurons, but not their projection to muscle, in a rat model of familial ALS. *PLoS ONE* **2**, e689.

Takahasi, K., Tanabe, K., Ohnuki, M., Narita, M., Ichisaka, T., Tomoda, K. and Yamanaka, S. (2007). Induction of pluripotent stem cells from adult human fibroblasts by defined factors. *Cell* **131**, 861-872.

Tamaki, T., Akatsuka, A., Ando, K., Nakamura, Y., Matsuzawa, H., Hotta, T., Roy, R. R. and Edgerton, V. R. (2002). Identification of myogenic-endothelial progenitor cells in the interstitial spaces of skeletal muscle. *J. Cell Biol.* **157**, 571-577.

Terada, N., Baracskay, K., Kinter, M., Melrose, S., Brophy, P. J., Boucheix, C., Bjartmar, C., Kidd, G. and Trapp, B. D. (2002). The tetraspanin protein, CD9, is expressed by progenitor cells committed to oligodendrogenesis and is linked to beta1 integrin, CD81, and Tspan-2. *Glia* **40**, 350-359.

Torrente, Y., Tremblay, J. P., Pisati, F., Belicchi, M., Rossi, B., Sironi, M., Fortunato, F., El Fahime, M., D'Angelo, M. G., Caron, N. J. et al. (2001). Intraarterial injection of muscle-derived CD34(+)Sca-1(+) stem cells restores dystrophin in mdx mice. *J. Cell Biol.* **152**, 335-348.

Trachtenberg, J. T. and Thompson, W. J. (1996). Schwann cell apoptosis at developing neuromuscular junctions is regulated by glial growth factor. *Nature* **379**, 174-177.

Trinidad, J. C., Fischbach, G. D. and Cohen, J. B. (2000). The Agrin/MuSK signaling pathway is spatially segregated from the neuregulin/ErbB receptor signaling pathway at the neuromuscular junction. *J. Neurosci.* **20**, 8762-8770.

van der Putten, H., Wiederhold, K. H., Probst, A., Barbieri, S., Mistl, C., Danner, S., Kauffmann, S., Hofele, K., Spooren, W. P., Ruegg, M. A. et al. (2000). Neuropathology in mice expressing human alpha-synuclein. *J. Neurosci.* **20**, 6021-6029.

Vanderwinden, J. M., Rumessen, J. J., De Laet, M. H., Vanderhaeghen, J. J. and Schiffmann, S. N. (1999). CD34+ cells in human intestine are fibroblasts adjacent to, but distinct from, interstitial cells of Cajal. *Lab. Invest.* **79**, 59-65.

VanSaun, M., Herrera, A. A. and Werle, M. J. (2003). Structural alterations at the neuromuscular junctions of matrix metalloproteinase 3 null mutant mice. *J. Neurocytol.* **32**, 1129-1142.

Weis, J., Fine, S. M., David, C., Savarirayan, S. and Sanes, J. R. (1991). Integration site-dependent expression of a transgene reveals specialized features of cells associated with neuromuscular junctions. *J. Cell Biol.* **113**, 1385-1397.

Wernig, M., Meissner, A., Foreman, R., Brambrink, T., Ku, M., Hochedlinger, K., Bernstein, B. E. and Jaenisch, R. (2007). *In vitro* reprogramming of fibroblasts into a pluripotent ES-cell-like state. *Nature* **448**, 318-324.

Wood, S. J. and Slater, C. R. (2001). Safety factor at the neuromuscular junction. *Prog. Neurobiol.* **64**, 393-429.

Zulli, A., Buxton, B. F., Black, M. J. and Hare, D. L. (2005). CD34 Class III positive cells are present in atherosclerotic plaques of the rabbit model of atherosclerosis. *Histochem. Cell Biol.* **124**, 517-522.

Zuo, Y., Lubischer, J. L., Kang, H., Tian, L., Mikesh, M., Marks, A., Scofield, V. L., Maika, S., Newman, C., Krieg, P. et al. (2004). Fluorescent proteins expressed in mouse transgenic lines mark subsets of glia, neurons, macrophages, and dendritic cells for vital examination. *J. Neurosci.* **24**, 10999-11009.